1106–1117 *Nucleic Acids Research, 2012, Vol. 40, No. 3* *Published online 7 October 2011*
doi:10.1093/nar/gkr837

Phosphorylation of SRSF1 is modulated by replicational stress

Valentina Leva[1], Serena Giuliano[2], Anna Bardoni[2], Serena Camerini[3], Marco Crescenzi[3], Antonella Lisa[1], Giuseppe Biamonti[1] and Alessandra Montecucco[1,*]

[1]Istituto di Genetica Molecolare, Consiglio Nazionale delle Ricerche, 27100 Pavia, [2]Dipartimento di Biochimica, Università di Pavia, 27100 Pavia and [3]Dipartimento di Biologia Cellulare e Neuroscienze, Istituto Superiore di Sanità, 00161 Roma, Italy

Received August 19, 2011; Revised September 19, 2011; Accepted September 20, 2011

ABSTRACT

DNA ligase I-deficient 46BR.1G1 cells show a delay in the maturation of replicative intermediates resulting in the accumulation of single- and double-stranded DNA breaks. As a consequence the ataxia telangiectasia mutated protein kinase (ATM) is constitutively phosphorylated at a basal level. Here, we use 46BR.1G1 cells as a model system to study the cell response to chronic replication-dependent DNA damage. Starting from a proteomic approach, we demonstrate that the phosphorylation level of factors controlling constitutive and alternative splicing is affected by the damage elicited by DNA ligase I deficiency. In particular, we show that SRSF1 is hyperphosphorylated in 46BR.1G1 cells compared to control fibroblasts. This hyperphosphorylation can be partially prevented by inhibiting ATM activity with caffeine. Notably, hyperphosphorylation of SRSF1 affects the subnuclear distribution of the protein and the alternative splicing pattern of target genes. We also unveil a modulation of SRSF1 phosphorylation after exposure of MRC-5V1 control fibroblasts to different exogenous sources of DNA damage. Altogether, our observations indicate that a relevant aspect of the cell response to DNA damage involves the post-translational regulation of splicing factor SRSF1 which is associated with a shift in the alternative splicing program of target genes to control cell survival or cell death.

INTRODUCTION

DNA replication can pose serious threats to the integrity of genetic information originating both from errors of DNA polymerases and from the unwinding of the double helix that produces highly unstable stretches of single-stranded DNA. While leading strand replication is the continuous extension of one primer in the 5′ to 3′ direction, lagging strand replication occurs in a discontinuous manner through the synthesis and joining of short DNA segments, called Okazaki fragments (1). On the lagging strand, the polymerase α/primase complex synthesizes RNA/DNA primers that are then extended by DNA polymerase δ (pol δ) to the full length of Okazaki fragments. When encountering the 5′-end of a downstream Okazaki fragment, pol δ strand-displaces the primer into a single-strand flap that is processed by flap endonuclease 1 (Fen1) to form a nick [reviewed by (2)]. Eventually the nick is sealed by DNA ligase I (LigI) to yield the continuous double-stranded DNA (3). A SV40 transformed cell line named 46BR.1G1 has been established from a patient with a genetic syndrome due to replicative LigI haploinsufficiency (4). These cells encode a mutated version of the enzyme in which the conserved Arg 771 in the catalytic fragment is replaced with a Trp residue. This mutation slows down the second step of the ligation reaction allowing the accumulation of nicked DNA-adenylated intermediates (5). As a consequence 46BR.1G1 cells show a delayed maturation of Okazaki fragments, which results in the accumulation of single- and double-stranded DNA breaks (6,7). These defects can be corrected by over-expressing the wild-type enzyme as in clone 7A3 (7). Notably, the replication-dependent DNA damage in LigI-deficient cells fails to halt cell-cycle progression and to induce apoptosis. Actually, 46BR.1G1 cells display only a moderate delay in cell-cycle progression and do not activate the S-phase specific ATR/Chk1 checkpoint pathway that also monitors the execution of mitosis, while the ATM/Chk2 pathway is constitutively activated at basal level (7,8). Thus, it is presently unknown which is the strategy used by LigI-deficient cells to cope with this higher basal level of DNA damage.

*To whom correspondence should be addressed. Tel: +39 0382 546351; Fax: +39 0382 422286; Email: montecucco@igm.cnr.it

Splicing is the process by which intronic sequences are removed from pre-mRNAs to form mature mRNA molecules. This reaction is carried out by a complex macromolecular machine, the 'spliceosome', which consists of five small nuclear ribonucleoproteins particles (snRNPs) and a large number of non-snRNP-splicing factors (9). With the exception of the first and last di-nucleotides at the intron boundaries, splice sites correspond to short, loose consensus sequences. This flexibility of the spliceosome in recognizing different splice site sequences has been exploited during evolution for an important regulatory phenomenon, known as alternative splicing, by which different combinations of splice sites can be joined to each other, resulting in the synthesis of several structurally and functionally distinct protein isoforms thereby enabling large proteomic complexity from a limited number of genes [reviewed by (10)]. The vast majority (~90%) of human gene transcripts undergo at least one alternative splicing event. Usually, the interplay of *cis*-acting sequences and *trans*-acting factors modulates the splicing of regulated exons. Key *cis*-acting sequence elements in splicing regulation are splicing enhancers and silencers, either exonic or intronic, which respectively promote or inhibit exon inclusion. In general, splicing enhancers are bound and activated by serine/arginine-rich proteins (SR proteins), which comprise a family of structurally related proteins that are highly conserved throughout evolution and are involved in both constitutive and alternative splicing regulation (11). The activity of SR proteins in alternative splicing can be antagonized by another group of RNA-binding proteins, the hnRNP proteins (heterogeneous nuclear ribonucleoprotein).

Owing to its broad impact on gene expression programs, alternative splicing provides an ideal means to modulate gene expression to the needs of the cells in response to stressing conditions. This is even more evident if one considers that alternative splicing events are direct targets of signal transduction cascades. Thus, impacting on specific signaling pathways could have drastic effects on splicing of specific pre-mRNAs, sometimes giving rise to protein isoforms with unique properties upon stress stimuli.

SRSF1 (12) is the prototypical SR protein. In addition to its role as a specific splicing regulator, SRSF1 participates in other cellular processes as genome maintenance and cell-cycle progression (13,14). Notably, SRSF1 has been recently shown to regulate an alternative splicing network linking cell-cycle control to apoptosis (15).

In this study we use 46BR.1G1 cells as a model system to study the response to chronic replication-dependent DNA damage. Starting from a proteomic approach we demonstrate that SRSF1 phosphorylation is regulated during the DNA damage response, shifting the alternative splicing pattern of target genes to control cell survival.

MATERIAL AND METHODS

Drugs, cells lines and cell treatments

Human SV40-transformed fibroblast MRC-5V1 and 46BR.1G1 (European Collection of Cell Cultures # CB2577) were maintained in monolayer culture in DMEM supplemented with 10% FBS, 4 mM glutamine and 50 μg/ml gentamicin (Sigma). 46BR.1G1 derivative 7A3 (7) was grown in complete DMEM supplemented with 300 μg/ml geneticin (Sigma). To inhibit ATM kinase activity 46BR.1G1 cells were treated with 2 mM caffeine (Sigma) or 10 μM KU-55933 for 24 h. To induce the DNA damage response MRC-5V1 were treated with 100 μM etoposide (Sigma) or 2 μg/ml aphidicolin (Sigma) for 3 h as previously described (16). For UV treatment MRC-5V1 were exposed to UV-C radiations (2, 5, 10 and 20 J/m^2) and collected after 3 h.

2D polyacrylamide gel electrophoresis and mass spectrometry

Protein concentration was determined at 280 nm using the 2D Quant Kit (GE Healthcare). Proteins from total cell extracts were precipitated with trichloroacetic acid and run on non-linear (NL) pH 3–10 or linear pH 4–7 gradient range IPG gel strips (length 18 cm in both cases) (GE Healthcare). Strips were re-hydrated in the swelling solution (8 M urea, 4% w/v CHAPS, 65 mM DTE, 0.8% v/v carrier ampholytes and bromophenol blue) containing 1.3 mg of proteins and focused with the Ettan IPGphor system (GE Healthcare). After focusing reduction/alkylation steps were performed in rehydration buffer (6 M urea, 2% w/v SDS, 50 mM Tris pH 6.8, glycerol 30%) containing 2% w/v DTE and 2.5% w/v IAA respectively. The IPG strips were loaded onto 20×18 cm 9–16% or constant 9% SDS–polyacrylamide gels as previously described (17). The 2DE gels were stained with Coomassie Blue Silver colloidal (18). Protein patterns were scanned with the VersaDoc imaging system (BioRad) and analyzed with the PDQuest Version 7.2 software (BioRad). Only spots with high quality (>30) were selected. For each cell line (six replicas) the PDQuest software originated a reference gel (master gel) including protein spots present in all six gels. From comparison between the master gels a virtual image (higher master gel) was created comprehensive of all matched spots. Standard statistical test [one-way ANOVA and Bonferroni *post hoc* test performed using STATA 10 (19)] have been performed to highlight significant spots ($P < 0.05$) for mass spectrometry analyses. For protein identification, spots of interest were excised from SDS–polyacrylamide gel electrophoresis (PAGE) gels, washed with 25 mM ammonium bicarbonate, dried with acetonitrile and digested overnight with modified sequencing-grade trypsin (Promega Corporation, Madison, WI, USA) as described elsewhere (20). Peptide mixture was analyzed by matrix assisted laser desorption ionization time of flight (MALDI–TOF–MS): 1 ml of the supernatant of the digestion was spotted in the MALDI plate using the dried droplet technique and α-cyano-4-hydroxycinnamic acid (Sigma-Aldrich) as matrix. All analyses were performed using a Voyager-DE STR (Applied Biosystems, Framingham, MA, USA) TOF spectrometer operating in the delayed extraction mode. Peptides were measured in the mass range from 750 to 4000 Da; all spectra were internally calibrated and

processed via the Data Explorer software (Applied Biosystems, Framingham, MA, USA). Proteins were unambiguously identified by mass fingerprint searching in a comprehensive non-redundant protein database (Swiss Prot) using Mascot (www.matrixscience.com) (21). The search parameters were: enzymatic digestion by trypsin, complete carbamydomethylation on cysteine residues, variable oxidation of methionine, and 50 ppm mass tolerance.

Cell extract and western blotting

Cell lysate, nuclear extracts and chromatins were prepared as previously described (22). For 2D western blotting, cells were harvested in lysis buffer (7 M urea, 2 M Thiourea and 4% CHAPS) containing protease and phosphatase inhibitors cocktail (Roche), sonicated and then incubated with DNAse I (Roche) 0.05 U/μl for 10 min in ice (total cell extract). After centrifugation the sample (200 μg) was desalted through ZebaTM micro Desalt Spin Column (Pierce) and loaded on linear pH 3–10 gradient IPG Strip in IEF buffer [8 M urea, 2 M Thiourea, 2% CHAPS, 50 mM DTT, 0.2% v/v, BioRad Bio-lyte 3/10 ampholyte, 0.001% (w/v) Bromophenol Blue]. All the reagents for 2D PAGE were from BioRad. 2D gel electrophoresis was performed in Mini-Protean 2D (BioRad) according to manufacturer's instructions. First dimension was carried out at 400 V end voltage. Then IPG Strips were incubated in equilibration buffer [6 M urea, 0.375 M Tris–HCl pH 8.8, 2% SDS, 20% glycerol, 2% (w/v) DTT] for 20 min. For the second dimension, IPG Strips were loaded on a 10% (w/v) SDS–PAGE overlaid with 0.5% (w/v) Overlay Agarose (BioRad) and run at 200 V. For protein dephosphorylation $4.5–5 \times 10^6$ cells were scraped into 150 μl of NP-40 lysis buffer (50 mM Tris–HCl pH 8.0, 150 mM NaCl, 1% NP-40, 100 μg/ml phenylmethylsulfonyl fluoride and protease inhibitors cocktail) and sonicated. After centrifugation, the supernatant was incubated with 500 U of alkaline phosphatase (Roche) for 1 h at 37°C. Cell extracts were analyzed by 1D and 2D western blotting with the following primary antibodies: anti-Splicing Factor-2 (mAb96) from Invitrogen Corporation, anti-MEK2 (clone 96) from BD Bioscience, anti-Actin (2Q1055), anti-PCNA (PC10) and anti-Orc2 (clone 3G6) from Santa Cruz Biotechnology, anti-α-tubulin from Sigma, anti-phospho-SR-proteins (mAb104) from hybridoma cells supernatant (ATCC # CRL-2067). Primary antibodies were revealed with peroxidase-conjugated goat anti-mouse, anti-rabbit or anti-rat antibodies (Jackson Immunoresearch Laboratories) and enhanced chemiluminescence system (Super Signal West Pico Pierce or Super Signal West Dura Extended).

RT–PCR

An amount of 1 μg of DNAse I-treated total RNA was retro-transcribed with d(T)18 and MuLV Reverse Transcriptase (GeneAmp RNA PCR kit, Applied Biosystem). An aliquot (1 μl) was PCR amplified with the following pairs of primers: SF2_A_fw (5′-AGGAGG ATTGAGGAGGATCAG-3′) and SF2_B_rev (5′-CGCT CCATGAATCCTGGTAA-3′); Ron_2507 (5′-CCTGAA TATGTGGTCCGAGACCCCCAG-3′) and Ron_2991 (5′-CTAGCTGCTTCCTCCGCCACCAGTA-3′); Caspase 9_fw (5′-GCTCTTCCTTTGTTCATCTCC-3′) and Caspase 9_rev (5′-CATCTGGCTCGGGGTTAC TGC-3′); GAPDH_fw (5′-ACCACAGTCCATGCCATC AC-3′) and GAPDH_rev (5′-TCCACCACCCTGTTGC TGTA-3′). The intensity of the amplification bands was quantified with NIH Image J software (version 1.43). Real time quantitative PCR was performed as previously described (23) with the following sets of primers: SF2_tot_for (5′-CTCCAAGTGGAAGTTGGCAGGAT T-3′) and SF2_tot_rev (5′-CTCCAAGTGGAAGTTGG CAGGATT-3′); HP0_for (5′-ATGCCCAGGGAAGAC AGGGCG-3′) and HP0_rev (5′-CGAAGGGACATGCG GATCTGCTGC-3′).

RESULTS

Proteomic analysis of LigI-deficient 46BR.1G1 cells

In order to gain insights into the mechanisms that allow 46BR.1G1 cell proliferation in the presence of a high level of replication-dependent DNA damage we compared the proteomic profiles of 46BR.1G1 and of the derivative 7A3 clone stably expressing the human LigI cDNA that corrects the 46BR.1G1 phenotype (7). By 2D gel electrophoresis analysis (six replicas) we identified 62 spots with statistically different abundance ($P < 0.05$) in the two cell lines. Proteins in the 62 spots were identified by mass spectrometry (Supplementary Table SI and Figure 1A): 59 spots corresponded to single proteins while three spots contained a mix of two proteins. As shown in Figure 1B, the great majority of the identified proteins is involved in the stress response i.e. protein folding and stabilization (13 spots), protein catabolism (four spots) positive and negative regulators of apoptosis (five spots), signal transduction (seven spots) and mitochondrial proteins and proteins involved in cell redox homeostasis (seven spots). We also found proteins (six spots) involved in cytoskeletal organization and cell motility. Unexpectedly, a relevant fraction of protein (six spots) differentially expressed in LigI-deficient cells consists of alternative splicing regulators among which heterogeneous nuclear ribonucleoproteins hnRNP C, hnRNP D, hnRNP H and the prototypical SR factor SRSF1 (already known as splicing factor 2/alternative splicing factor).

LigI-deficiency perturbs the phosphorylation of SRSF1

Several reports have recently suggested a role of SRSF1 in genome integrity and chromatin organization by preventing the formation of R-loops and by modulating the association of heterochromatin protein 1 (HP1) with chromatin (24,25). Moreover SRSF1 has been found to be part of an alternative splicing network that links cell-cycle control to apoptosis (15). Thus, we decided to verify whether SRSF1 was indeed differentially expressed in LigI deficient cells as suggested by the proteomic analysis. However, western blot analysis (Figure 2A) evidenced only a moderate increase (1.26 ± 0.03-fold) in

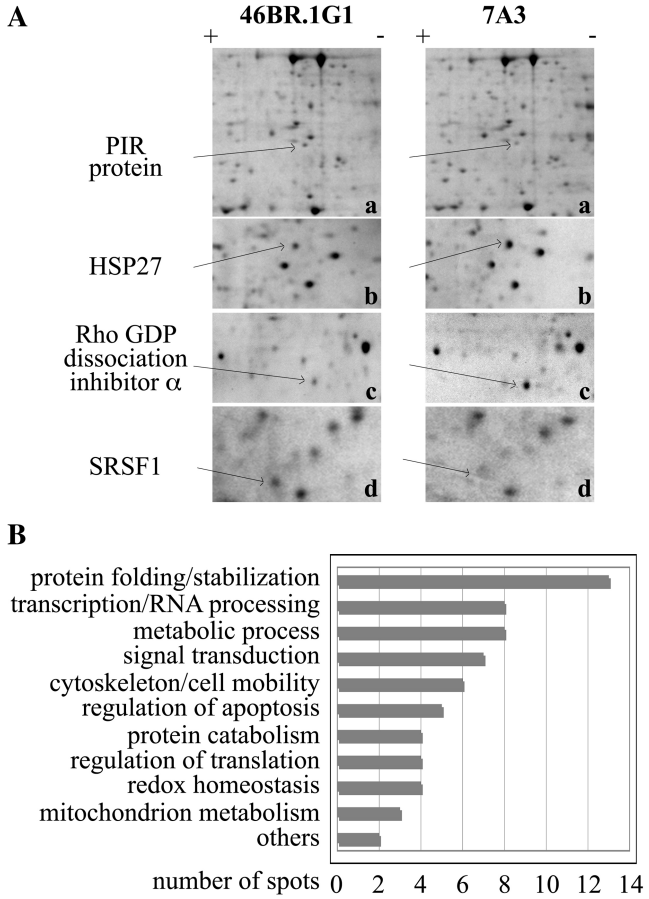

Figure 1. Proteins with differential expression in 46BR.1G1 and 7A3 cells as shown by 2D electrophoresis. (**A**) Representative 2D gel analysis of 46BR.1G1 LigI-defective (left) and 7A3 cells expressing the wild-type LigI cDNA (right). Proteins were focused on IPG strip non-linear pH 3-10 (a) or linear pH 4-7 (b–d) gradient ranges and then separated into 9–16% (a) or constant 9% (b–d) polyacrylamide gels. Gels were stained with Coomassie Blue Silver colloidal. Corresponding expanded areas of gels for the two cell lines are shown. Arrows point to spots that reproducibly showed volume variations in six independent replicas. Proteins in the indicated spots were eluted and identified by mass spectrometry (see 'Materials and Methods' section). (**B**) All spots with differential expressions were analyzed by mass spectrometry and assigned with the indicated functional categories.

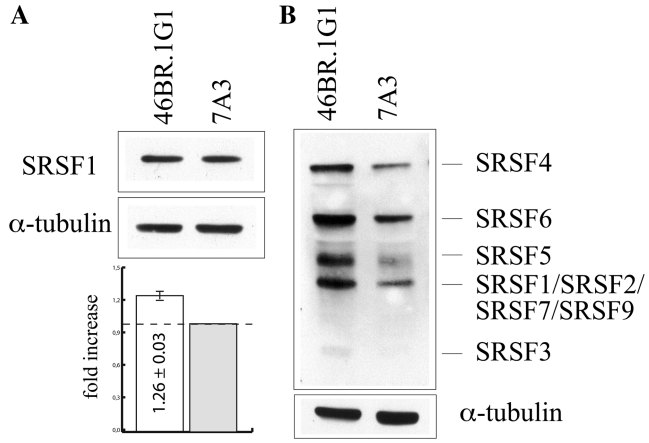

Figure 2. SRSF1 expression and phosphorylation of SR proteins in 46BR.1G1 and 7A3 cells. (**A**) Cell lysates from 46BR.1G1 and 7A3 cells were analyzed by western blotting with anti-SRSF1 (mAb96) and anti-α-tubulin antibodies. Quantification of the assay was performed by densitometric analysis with the NIH ImageJ 1.43 program. Bars show means ± SEM of three independent experiments. (**B**) Cell lysates from 46BR.1G1 and 7A3 cells were analyzed by western blotting with anti-SR-phosphoepitopes antibody (mAb104) and anti-α-tubulin antibody.

the level of SRSF1 in 46BR.1G1 compared to complemented 7A3 cells.

Similarly to all SR splicing factors, SRSF1 is heavily phosphorylated in the C-terminal domain formed by RS dipeptides (26); thus, we wondered whether the result of the proteomic analysis could reflect a different protein phosphorylation in the two cell lines. In an initial attempt to verify this hypothesis, we probed total cell extracts from LigI-deficient 46BR.1G1 and LigI-proficient 7A3 cells with the monoclonal antibody clone 104 that specifically recognizes phosphorylated SR proteins. As shown in Figure 2B, the intensity of the signal detected by mAb104 is considerably stronger in 46BR.1G1 than in 7A3 suggesting a higher phosphorylation level of all SR factors in LigI deficient cells. In order to explore more in detail this aspect, we analyzed the 2D immunoblot profile of SRSF1. Actin, MEK2 and PCNA were used as internal reference of the isoelectric point (pI). Phosphorylation produces several isoforms of SRSF1 with different pI that can be resolved by 2D gel electrophoresis (Figure 3A). For a better comparison, the densitometric profile of SRSF1 is shown alongside each gel (Figure 3B). The SRSF1 isoforms distribution in control MRC-5V1 fibroblasts develops into two main pools: an acidic one (pool A), with a broad distribution in the range of pI from 4 to 5, and a more basic pool (pool B) focusing with a pI of 6.5/7. A drastically different distribution is detectable in 46BR.1G1 with a general shift toward lower pI. In particular, in LigI-deficient cells pool A extends between pI 3.5 and 5, while pool B migrates at the same pI as MEK2 (5.5/6). Remarkably the migration profile observed in normal fibroblasts is re-established upon stably expression of wild-type LigI in 46BR.1G1 as indicated by the 2D western blotting of 7A3 cells extract. This finding strongly supports the conclusion that SRSF1 phosphorylation is modulated in response to the DNA damage elicited by LigI deficiency.

In 46BR.1G1 cells the ATM kinase is constitutively phosphorylated on serine 1918 (7) and this activation is reverted in 7A3 cells. We wondered whether or not the change in the 2D gel profile of SRSF1 could be triggered by the chronic activation of the DNA damage checkpoint. To verify this hypothesis, we analyzed the 2D immunoprofile of SRSF1 in 46BR.1G1 grown for 24 h in 2 mM caffeine, an inhibitor of checkpoint kinases. As shown in Figure 3A and B, upon treatment with caffeine the 2D gel profile of SRSF1 shifts toward higher pI although the migration of pool B observed in normal fibroblasts is not re-established. To prove that the acidic pool of SRSF1 observed in 46BR.1G1 cells was indeed due to protein hyper-phosphorylation, the cell extract was incubated with alkaline phosphatase before

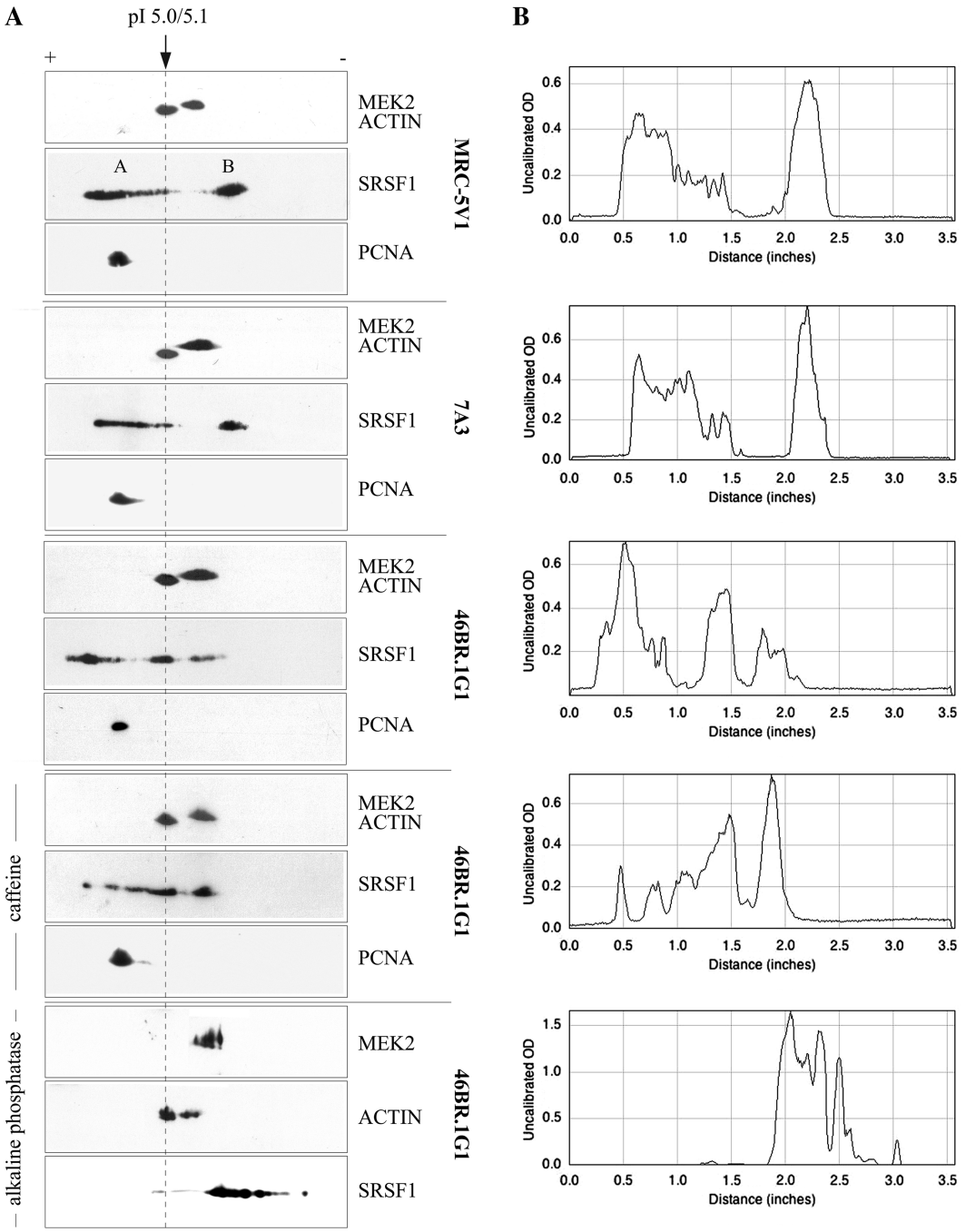

Figure 3. SRSF1 is hyperphosphorylated in 46BR.1G1 cells. (**A**) 2D western blot analyses of total extracts from MRC-5V1, 7A3 and 46BR.1G1 cells with anti-SRSF1, anti-MEK2, anti-actin and anti-PCNA antibodies. A total extract was also prepared from 46BR.1G1 cells after 24 h incubation in 2 mM caffeine to inhibit checkpoint kinases activity. The isoelectric profile of SRSF1 was also determined after incubation of 46BR.1G1 cell extract with alkaline phosphatase. Caffeine and alkaline phosphatase treatments are indicated alongside the gel. (**B**) The signal of SRSF1 was quantified with the NIH ImageJ 1.43 version program: the *x*-axis represents the distance from the anode and the *y*-axis measures the pixel intensities.

2D western blot analysis. As shown in Figure 3A and B (bottom plot), the acidic pool disappeared after protein dephosphorylation and most SRSF1 focused in a few spots with a pI > 6.

LigI-deficiency affects localization and activity of SRSF1

The extensive serine phosphorylation of the RS domain is important to regulate the localization and activity of SRSF1. However, no difference was visible in the distribution of SRSF1 between 46BR.1G1 and 7A3 cells by immunofluorescence (data not shown). Thus, we investigated the distribution of SRSF1 in the same cell lines after biochemical cell fractionation. Cytoplasmic (S1), nucleoplasmic (S3) and chromatin enriched (P3) fractions were prepared from 46BR.1G1 and 7A3 cells as previously described (22). Extracts were then analyzed in western blotting; MEK2 and Orc2 were used as markers

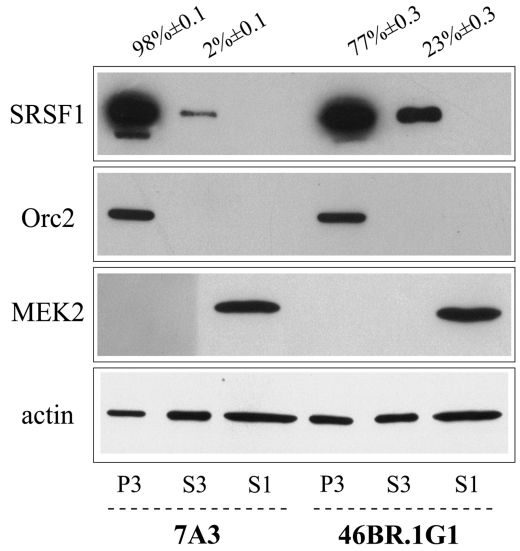

Figure 4. The nucleoplasmic fraction of SRSF1 increases in 46BR.1G1 cells. Exponentially growing 46BR.1G1 and 7A3 cells were fractionated to obtain the chromatin enriched (P3), nucleoplasmic (S3) and cytoplasmic (S1) fractions. Cell fractions were analyzed by western blotting with anti-SRSF1, anti-Orc2, anti-MEK2 and anti-actin monoclonal antibodies. The percentage of SRSF1 in P3 and S3 fractions is the mean of two independent experiments.

of the cytoplasmic and chromatin fraction, respectively. As shown in Figure 4, under these experimental conditions SRSF1 is exclusively found in the nuclear fractions of both cell lines. However, a difference in the subnuclear distribution of SRSF1 is clearly visible, and the fraction of the protein in the soluble nucleoplasm increases from 2% in 7A3 cells to ~20% in 46BR.1G1.

It has been shown that transcription inhibition leads to translocation of SRSF1 from the nucleoplasm to nuclear speckles (27) indicating that the nucleoplasmic fraction comprises the pool of SRSF1 involved in pre-mRNA processing. Thus, one can predict that an increased amount of SRSF1 in the nucleoplasmic fraction of 46BR.1G1 cell could affect the alternative splicing profile of target gene transcripts. One of the best-characterized targets of SRSF1 is Ron proto-oncogene, which encodes the human receptor for the macrophage-stimulating protein (MSP) (28). SRSF1 controls the choice between skipping versus inclusion of Ron exon 11 (Figure 5A): high levels of SRSF1 induce skipping of exon 11 and the production of ΔRon. RT–PCR analysis (Figure 5B) indicates that the full length Ron isoform prevails in 7A3 cells while ΔRon increases in 46BR.1G1 cells. SRSF1 also functions as regulator of caspase-9 (Casp9) pre-mRNA processing (15). Two splice variants (pro-apoptotic Casp9a and anti-apoptotic Casp9b) are encoded by the *Caspase 9* gene through alternative splicing of a cassette composed of exons 3, 4, 5 and 6 (Figure 5A). It has been recently shown that phosphorylation of the RS domain of SRSF1 is critical in promoting the Casp9b-splicing variant (29). In agreement with these observations RT–PCR analyses show a reduction of Casp9a/Casp9b ratio in 46BR.1G1 versus 7A3 cells (Figure 5B). Therefore, the alternative splicing profiles of SRSF1 target genes differ in 46BR.1G1 versus 7A3 cells in parallel with the increased level in the nucleoplasm and phosphorylation of SRSF1. This conclusion is also supported by the analysis of two additional splicing events controlled by SRSF1, namely *RPS6KB1* and *MKNK2* genes (Supplementary Figure S1) (30).

In order to understand the role of checkpoint activation in the difference of splicing profiles between 46BR.1G1 and 7A3 cells, we decided to investigate the effect of caffeine, a general inhibitor of checkpoint kinases, and of KU-55933, that specifically inhibits the ATM pathway (31). Therefore, 46BR.1G1 were incubated for 24 h in the presence of caffeine or KU-55933 before RNA purification. The RT–PCR analyses in Figure 5C show that both inhibitors affect Ron/ΔRon and Casp9a/Casp9b ratios in 46BR.1G1 cells reverting them to values comparable to those observed in 7A3 cells. No effect is detectable in 7A3 cells expressing the wild-type LigI (data not shown). These data indicate that the LigI defect, which results in a high level of replicative DNA damage, impacts the alternative splicing of SRSF1 target transcripts in ATM-dependent manner. The different phosphorylation status of SR proteins and of SRSF1 in particular between 46BR.1G1 and 7A3 cells (Figures 2 and 3) seems to be relevant for this event.

Different DNA damages perturb SRSF1 phosphorylation

The results in Figure 3 indicate that SRSF1 is regulated at the post-translational level in response to the increased basal level of endogenous DNA damage observed in LigI-deficient cells. We wondered whether the acute exposure to exogenous sources of DNA damage could affect the protein phosphorylation as well. To answer this question we have investigated by 2D gel western blotting the isoelectric profile of SRSF1 in MRC-5V1 human fibroblasts before and after treatment with three different DNA damaging agents inducing specific DNA damage responses: ultraviolet irradiation (UV), etoposide and aphidicolin. Contrary to LigI-deficiency all these DNA damages induce cell-cycle arrest although by different mechanisms. UV and aphidicolin induce stalling of replication forks that need to be stabilized by the ATR-dependent checkpoint pathway (32). Etoposide is a Topo II poison that induces both ATR- and ATM-dependent checkpoint pathways (16). Human MRC-5V1 fibroblasts were treated with the different agents as described in 'Materials and Methods' section, after 3 h cells were lysed and total extracts were run on 2D gels. As shown in Figure 6 all these treatments affect the isoelectric profile of SRSF1. However contrary to what observed in LigI-deficient cells they promote a shift toward higher isoelectric points and the disappearance of the acidic tail detectable in the extract of untreated cells. Thus SRSF1 phosphorylation is modulated in response to a wide set of endogenous and exogenous agents that threat genome integrity. Notably, in response to UV irradiation there is also a drastic reduction in the abundance of the basic pool B. Altogether these results indicate the SRSF1 is a target of post-translational modifications triggered by different types of DNA damages.

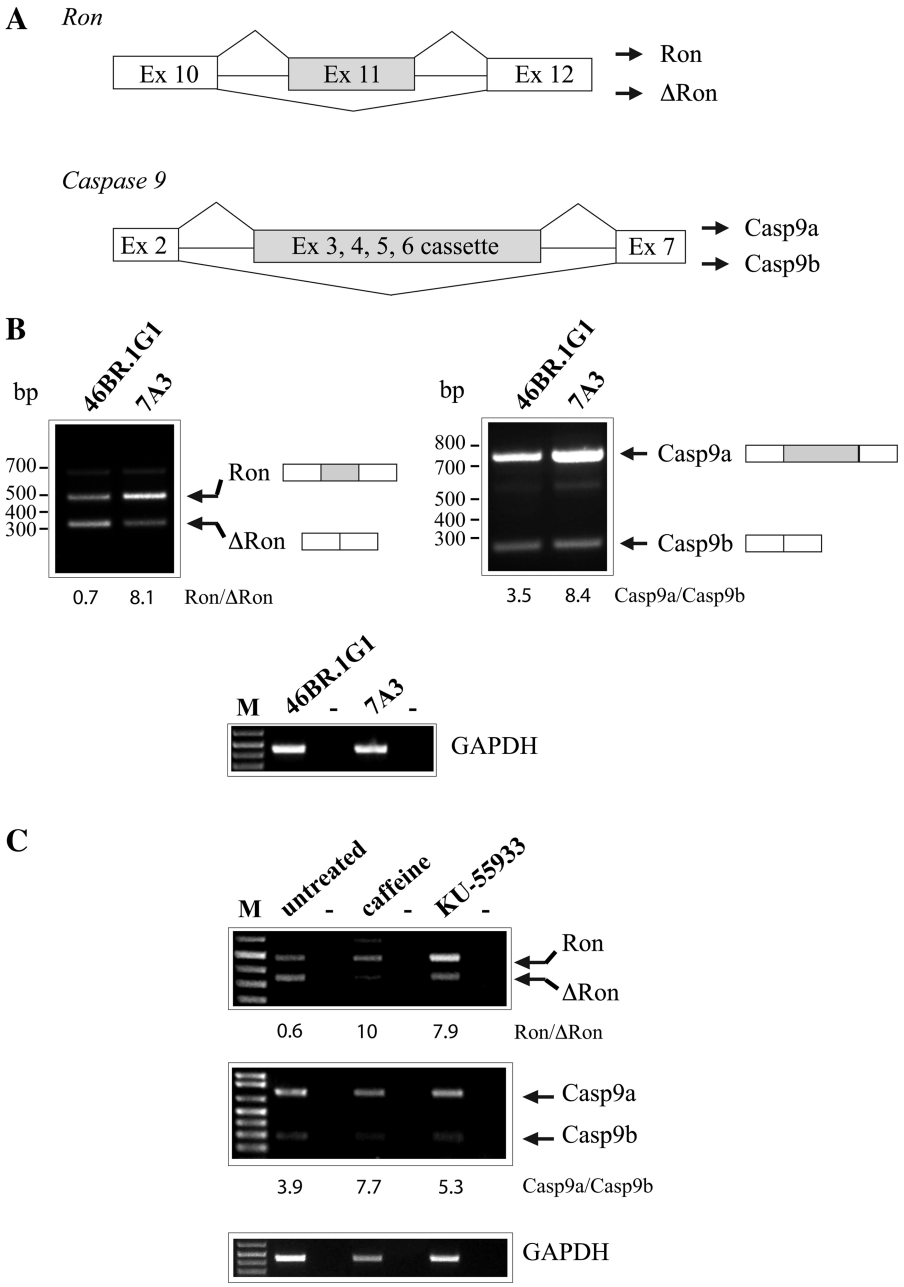

Figure 5. The alternative splicing of SRSF1 target genes Ron and caspase 9 is altered in LigI-deficient cells. (**A**) Schematic representation of alternative splicing in Ron and Caspase 9 transcript. (**B**) Total RNAs from 46BR.1G1 and 7A3 cell lines were analyzed by RT–PCR with Ron primers 2507 and 2991 annealing to exon 10 and exon 12 respectively, with Caspase 9_fw and Caspase 9_rev primers annealing to exon 2 and exon 7 respectively, and with specific primers for the GAPDH control mRNA. The Ron/ΔRon and Caspase9a/Caspase9b ratios were calculated on the basis of the intensity of the amplification bands quantified with the NIH ImageJ 1.43 program and are indicated below each lane. (**C**) The same ratios were calculated in 46BR.1G1 untreated and treated for 24 h with 2 mM caffeine or 10 μM KU-55933. M, DNA size markers.

LigI-deficiency affects post-transcriptional control of SRSF1 transcripts

In spite of the slight increase of SRSF1 protein (Figure 2A) RT-qPCR analysis does not reveal a statistically significant difference in the amount of SRSF1 transcript between 46BR.1G1 and 7A3 cells (data not shown). We have recently shown that the level of SRSF1 protein can be controlled through an alternative splicing event involving an intron in the 3′-UTR region (3′-UTR intron) of the gene. Splicing of this intron results in a mRNA molecule (NMD+ RNA, Figure 7A) in which the natural stop codon is recognized as a premature termination codon (PTC) (23) leading to mRNA degradation by the nonsense mediated RNA decay (NMD) pathway after the first round of translation. Based on this knowledge, we have compared the splicing profile of the 3′-UTR intron in MRC-5V1 control fibroblasts, 46BR.1G1 and complemented 7A3 cells. As shown in

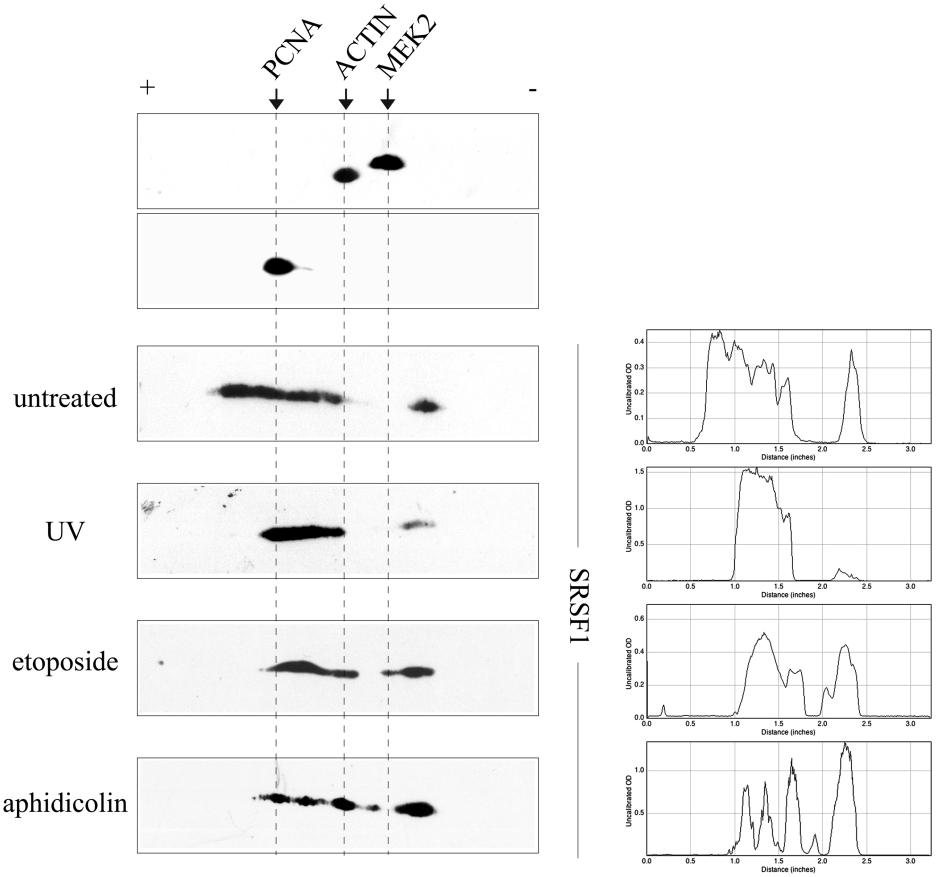

Figure 6. Phosphorylation of SRSF1 changes in response to DNA damaging agents. Total cell extracts from MRC-5V1 human fibroblasts untreated and treated with the indicated DNA damaging agents were analyzed by 2D western blotting. Filters were incubated with anti-SRSF1, anti-PCNA, anti-MEK2 and anti-actin monoclonal antibodies. The densitometric profile of SRSF1 is shown alongside each gel. The *x*-axis represents the distance from the anode and the *y*-axis the pixel intensity (NIH ImageJ 1.43).

Figure 7B, the band corresponding to NMD+ RNA accounts for ~5% of the total signal in control human fibroblasts (MRC-5V1) and in cells stably expressing wild-type LigI (7A3) while it is barely detectable in 46BR.1G1 cells. Taking into accounts the different length of the two amplification bands (100 and 1000 nt respectively for the NMD+ and full-length splicing isoforms) the RT–PCR analysis indicates that in molar terms the NMD+ mRNA represents ~30% of total SRSF1 RNA in 7A3 cells. Thus, the different splicing of SRSF1 transcript could explain the difference in protein level observed in Figure 2. Interestingly, a change in the splicing profile of SRSF1 transcript is elicited also by UV light and results in an increased splicing of the 3′-UTR intron in a dose-dependent manner (Figure 7C and D). In the considered time interval (3 h after UV irradiation) we did not detect significant variation in the amount of SRSF1 protein (data not shown).

DISCUSSION

DNA ligase I deficiency in 46BR.1G1 cells severely impacts the maturation of newly synthesized DNA (7). This defect results in an increased level of endogenous DNA damage as revealed by phosphorylation of the histone variant H2AX and the formation of γH2AX foci, which are markers of DSBs (33). Although important, the LigI defect in 46BR.1G1 cells does not block cell-cycle progression and elicits only a moderate activation of the checkpoint pathway identified by ATM/Chk2 kinases. Notably, the expression of ectopic wild-type LigI (7A3 cells) reverses all these effects (7).

This peculiar phenotype of 46BR.1G1 cells makes them a suitable system to investigate the strategies used by the cells to cope with an increased endogenous level of DNA replication dependent DNA damage that, nevertheless, is compatible with survival and proliferation. As a first attempt to address this issue, we applied a proteomic approach aimed at identifying proteins differentially expressed and/or post-translationally modified in LigI-deficient cells compared to normal MRC-5V1 fibroblasts and to 7A3 cells. This analysis identified a small set of proteins most of which appear to be involved in the stress response and in the organization of the cytoskeleton. Interestingly, a fraction of the identified proteins consists of factors with a role in alternative splicing of gene transcripts (see the list in Supplementary Table S1). A still growing body of experimental evidences implicates splicing regulators in the DNA damage response (DDR) and in genome stability. These factors appear to act by

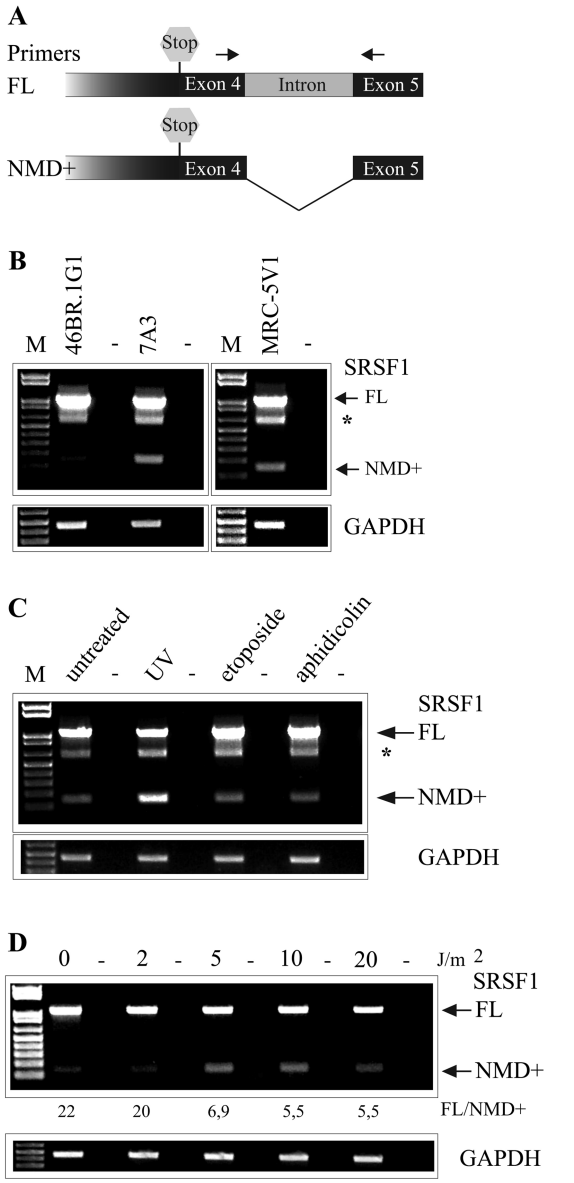

Figure 7. The alternative splicing of SRSF1 is modified in 46BR.1G1 cells and is regulated in response to UV-light. (**A**) Schematic representation of alternative splicing in the 3′-UTR of SRSF1 transcripts. FL, full-length transcript of SRSF1; NMD^+, splicing variant associated with the non-sense mediated mRNA decay pathway. (**B**) Total RNA from 46BR.1G1, 7A3 and MRC.5V1 cell lines was analyzed by RT–PCR with primers that recognized both the FL and NMD^+ mRNAs of SRSF1 (arrows) and with specific primers for the GAPDH control mRNA. The asterisk indicates an unspecific PCR product. M, DNA size markers. (**C**) Total RNA from the MRC-5V1 control fibroblasts untreated or treated with different damaging agents was analyzed by RT–PCR (30 cycles) as in (B) with primers specific for SRSF1 and GAPDH mRNAs. The asterisk indicates an unspecific PCR product. (**D**) Total RNA was purified from MRC-5V1 3 h after exposure to the indicated UV doses and analyzed by RT–PCR (25 cycles) with primers that recognized both the FL and the NMD^+ mRNA of SRSF1 (arrows) and with primers for the GAPDH control mRNAs. M, DNA size markers. The ratio between FL and NMD^+ bands indicated under each line was calculated on the basis of the intensity of the bands quantified with the NIH ImageJ 1.43.

modulating, through alternative splicing, the activity of proteins that are critical for the proper cell response to stress, as for instance p53 and its regulator MDM2 (34). Moreover, some splicing factors have an additional and evolutionary conserved role in genome maintenance programs. Indeed, both in yeast and in mammals, a subset of splicing regulators is required to prevent the cotranscriptional generation of R-loops that are thought to results from inefficient processing of the nascent RNA molecule and the ensuing hybridization of the nascent transcript with the template DNA (RNA–DNA hybrid) (24,35). How R loops might lead to genome instability is unclear. One possibility is that the displaced ssDNA is more susceptible to DNA damage, ultimately leading to DSB formation and recombination. Alternatively, R-loops could represent DNA replication fork barriers and cause fork arrest and collapse (24). More recently, the link between RNA processing factors and DDR has been reinforced by genome-wide analyses for modulators of DNA damage signaling (36,37). Interestingly, the largest fraction of identified genes encodes proteins with functions in mRNA binding and processing including SFSR1 and hnRNP C that belong to the set of proteins selected by our proteomic approach.

DNA damage controls the phosphorylation profile of SRSF1

Because of these considerations, we decided to investigate more in detail the splicing regulator SRSF1. Interestingly, LigI deficiency only modestly affects the SRSF1 protein level (Figure 2), while it drastically perturbs the phosphorylation pattern as indicated by the altered electrophoretic mobility in 2D gel. The impact on protein phosphorylation is probably not specific to SRSF1 since western blot analysis with the mAb104, which recognizes phosphorylated SR factors, suggests a broad effect on the whole family of these splicing regulators. Thus, endogenous DNA damage in 46BR.1G1 cells appears to elicit a signaling pathway that targets proteins involved in pre-mRNA processing. In agreement with this interpretation we have observed that caffeine, which inhibits ATM and ATR kinases, partially prevents SRSF1 hyper-phosphorylation in 46BR.1G1 cells.

Alternative splicing is a predominant mechanism of gene expression regulation only in higher eukaryotes, specifically in mammals. However, basic components of the splicing machinery are conserved between yeast and human. Among yeast SR-like proteins, Npl3 displays some structural and functional features of SRSF1, including the presence of a non-canonical RRM (RNA Recognition Motif), the involvement in pre-mRNA processing, RNA export and translation. Both Npl3 and SRSF1 may auto-regulate their expression at the post-transcriptional level and undergo multiple phosphorylation events (38,39). Whether Npl3 inactivation induces genome instability is not presently known, but Npl3p mutants show hypersensitivity to DNA damaging agents (40). In agreement with our observations recent proteomic analyses have identified Npl3 as a target of DDR activated kinases Mec1 and Tel1 (41), homolog of mammalian ATR

and ATM kinases. Smolka and collaborators have demonstrated a DNA damage-dependent phosphorylation of Npl3 on serine 224 located in the non canonical RRM domain (RRM2) and adjacent to a heptapeptide ($SWQDLKD_{218}$) 100% conserved in the human protein and organized in an α helix. Interestingly, a putative phosphorylation site is predicted by the NetPhos 2.0 server (http://www.cbs.dtu.dk) at Ser 131 adjacent to the heptapeptide (residues 133–139) of human SRSF1 and a prediction of a chk1/chk2 phosphorylation site on Ser 131 is also provided by the PPSP site (http://ppsp.biocuckoo.org). In view of the importance that the heptapeptide has in the activity of SRSF1 in alternative splicing (42), it is conceivable to hypothesize important functional consequences of phosphorylation of nearby residues. However, so far we were unable to provide evidence of Ser 131 phosphorylation *in vivo*, by mass spectrometry analysis of the immunoprecipitated SRSF1. The relevance of our findings to genome-safeguard strategies is indicated also by the observation that post-translational modification of SRSF1 is modulated in response to a variety of exogenous DNA damaging agents. Remarkably, each stressing agent appears to induce a specific change in the electrophoretic mobility of the protein suggesting the activation of distinct signaling pathways.

Post-translational modification of SRSF1 and alternative splicing

As stated above the endogenous DNA damage in 46BR.1G1 cells affects the post-translational modification of a number of splicing regulators in addition to SRSF1, which hampers the possibility to establish a direct link between SRSF1 phosphorylation and changes in alternative splicing events. However, a number of evidences are consistent with this possibility. First of all, the increased phosphorylation is accompanied by the shift of SRSF1 from the nuclear pellet to the nucleoplasm (Figure 4) which suggests that a larger pool of protein is actually engaged in pre-mRNA processing in 46BR.1G1 cells compared to normal fibroblasts. Second evidence comes from the analysis of the splicing profile of Ron oncogene. We have previously shown that the level of SRSF1 controls splicing of Ron exon 11 and upregulation or over-expression of this splicing factor induces exon skipping (28). The modest difference in the SRSF1 level (1.3-fold) between 46BR.1G1 and 7A3 cells points to protein phosphorylation as the main cause of the drastically different splicing profile of exon 11 in the two cell lines. This conclusion is further supported by the observation that upon inhibition of checkpoint with caffeine or KU-55933 the splicing profile of Ron transcript in 46BR.1G1 cells becomes comparable to that observed in 7A3 cells. Similar consideration can be raised for the splicing profile of the caspase 9 RNA. Remarkably, the splicing variants of Ron and caspase 9 genes expressed in 46BR.1G1 cells are known to have anti-apoptotic activity which is consistent with the reported involvement of SRSF1 in anti-apoptotic pathways (15). On the contrary dephosphorylation of SR proteins after FAS activation enhances the execution of the apoptotic response (43). In line with this observation the reduction in the phosphorylation level of SRSF1 after UV-light treatment affects the alternative splicing of Ron exon 11 and reduces the expression of the anti-apoptotic ΔRon in a dose-dependent manner (Supplementary Figure S2).

Alternative splicing of SRSF1 transcripts is controlled by DNA damage

The 3′-UTR of the SRSF1 pre-mRNA contains an intron (3′-UTR-intron) that is normally retained in the mature transcript. Splicing of the 3′-UTR-intron leads to the production of the NMD+ transcript in which the natural stop codon is recognized as a premature stop codon and the mRNA degraded by the nonsense-mediated RNA decay (NMD) pathway. This alternative splicing event is one of the molecular mechanisms that control SRSF1 expression (44). We have recently shown that splicing of the 3′-UTR-intron is modulated during in vitro epithelial to mesenchymal transition (23). In epithelial cells most of SRSF1 pre-mRNA undergoes splicing of the 3′-UTR-intron with the production of the NMD sensitive mRNA. On the contrary, splicing of the intron is prevented in mesenchymal cells. In this manuscript we have shown that the ratio between the full length and the NMD^+ splicing isoform is also affected by DNA damaging agents. In particular it is perturbed by the replication dependent DNA damage mediated by LigI deficiency in 46BR.1G1 cell line. Among the exogenous DNA damaging agents tested in this study only UV-light drastically affects SRSF1 splicing and increases the production of the NMD+ mRNA in a dose dependent manner. It has been recently described a cotranscriptional mechanism for activating alternative pre-mRNA splicing after UV-irradiation that depends on hyperphosphorylation of the RNA polymerase II C-terminal domain and decreased rates of transcription elongation (45). Interestingly the fraction of genes that undergo a change in the alternative splicing after UV-light treatment is largely enriched in those genes that also show downregulated expression, suggesting that control of alternative splicing through its coupling with transcription is a key feature of the DNA-damage response. Moreover, these events appear not to be controlled by checkpoint pathways as indicated by the insensitivity to caffeine treatment. The fact that, differently form the other AS events considered in this study, splicing of the 3′-UTR intron is not modulated by ATM abrogators, caffeine and KU-55933 (data not shown), suggests the possibility that the elongation rate of RNA polymerase II may play a role in this event.

In conclusion, our observations, along with a growing list of evidences from other laboratories, are uncovering the existence of a DNA damage signal transduction pathway that directly regulates the splicing factors and suggest that the regulation of alternative splicing is a mechanism allowing cells to rapidly modify gene expression by adapting to new stress conditions.

SUPPLEMENTARY DATA

Supplementary Data are available at NAR Online: Supplementary Table 1, Supplementary Figures 1 and 2, Supplementary Methods, Supplementary Reference [30].

ACKNOWLEDGEMENTS

The authors thank Dr Mark O'Connor, KuDOS Pharmaceuticals LTD for the kind gift of KU-55933.

FUNDING

Associazione Italiana per la Ricerca sul Cancro to AM and GB, Fondazione CARIPLO and European Alternative Splicing Network to G.B.; Fondazione Adriano Buzzati Traverso postdoctoral fellowship to V.L. Funding for open access charge: AIRC.

Conflict of interest statement. None declared.

REFERENCES

1. Kornberg,A. and Baker,T.A. (1992) Replication mechanisms and operations. In Freeman,W.H. (ed.), *DNA Replication*, 2nd edn. University Science Books, New York.
2. Rossi,M.L., Purohit,V., Brandt,P.D. and Bambara,R.A. (2006) Lagging strand replication proteins in genome stability and DNA repair. *Chem. Rev.*, **106**, 453–473.
3. Tomkinson,A.E., Vijayakumar,S., Pascal,J.M. and Ellenberger,T. (2006) DNA ligases: structure, reaction mechanism, and function. *Chem. Rev.*, **106**, 687–699.
4. Barnes,D.E., Tomkinson,A.E., Lehmann,A.R., Webster,A.D. and Lindahl,T. (1992) Mutations in the DNA ligase I gene of an individual with immunodeficiencies and cellular hypersensitivity to DNA-damaging agents. *Cell*, **69**, 495–503.
5. Prigent,C., Satoh,M.S., Daly,G., Barnes,D.E. and Lindahl,T. (1994) Aberrant DNA repair and DNA replication due to an inherited enzymatic defect in human DNA ligase I. *Mol. Cell. Biol.*, **14**, 310–317.
6. Levin,D.S., McKenna,A.E., Motycka,T.A., Matsumoto,Y. and Tomkinson,A.E. (2000) Interaction between PCNA and DNA ligase I is critical for joining of Okazaki fragments and long-patch base-excision repair. *Curr. Biol.*, **10**, 919–922.
7. Soza,S., Leva,V., Vago,R., Ferrari,G., Mazzini,G., Biamonti,G. and Montecucco,A. (2009) DNA ligase I deficiency leads to replication-dependent DNA damage and impacts cell morphology without blocking cell cycle progression. *Mol. Cell. Biol.*, **29**, 2032–2041.
8. Vijayakumar,S., Dziegielewska,B., Levin,D.S., Song,W., Yin,J., Yang,A., Matsumoto,Y., Bermudez,V.P., Hurwitz,J. and Tomkinson,A.E. (2009) Phosphorylation of human DNA ligase I regulates its interaction with replication factor C and its participation in DNA replication and DNA repair. *Mol. Cell. Biol.*, **29**, 2042–2052.
9. Wahl,M.C., Will,C.L. and Luhrmann,R. (2009) The spliceosome: design principles of a dynamic RNP machine. *Cell*, **136**, 701–718.
10. Hartmann,B. and Valcarcel,J. (2009) Decrypting the genome's alternative messages. *Curr. Opin. Cell. Biol.*, **21**, 377–386.
11. Long,J.C. and Caceres,J.F. (2009) The SR protein family of splicing factors: master regulators of gene expression. *Biochem. J.*, **417**, 15–27.
12. Manley,J.L. and Krainer,A.R. (2010) A rational nomenclature for serine/arginine-rich protein splicing factors (SR proteins). *Genes Dev.*, **24**, 1073–1074.
13. Li,X., Wang,J. and Manley,J.L. (2005) Loss of splicing factor ASF/SF2 induces G2 cell cycle arrest and apoptosis, but inhibits internucleosomal DNA fragmentation. *Genes Dev.*, **19**, 2705–2714.
14. Li,X. and Manley,J.L. (2005) Inactivation of the SR protein splicing factor ASF/SF2 results in genomic instability. *Cell*, **122**, 365–378.
15. Moore,M.J., Wang,Q., Kennedy,C.J. and Silver,P.A. (2010) An alternative splicing network links cell-cycle control to apoptosis. *Cell*, **142**, 625–636.
16. Rossi,R., Lidonnici,M.R., Soza,S., Biamonti,G. and Montecucco,A. (2006) The dispersal of replication proteins after Etoposide treatment requires the cooperation of Nbs1 with the ataxia telangiectasia Rad3-related/Chk1 pathway. *Cancer Res.*, **66**, 1675–1683.
17. Di Poto,C., Iadarola,P., Bardoni,A.M., Passadore,I., Giorgetti,S., Cereda,C., Carri,M.T., Ceroni,M. and Salvini,R. (2007) 2-DE and MALDI-TOF-MS for a comparative analysis of proteins expressed in different cellular models of amyotrophic lateral sclerosis. *Electrophoresis*, **28**, 4320–4329.
18. Candiano,G., Bruschi,M., Musante,L., Santucci,L., Ghiggeri,G.M., Carnemolla,B., Orecchia,P., Zardi,L. and Righetti,P.G. (2004) Blue silver: a very sensitive colloidal Coomassie G-250 staining for proteome analysis. *Electrophoresis*, **25**, 1327–1333.
19. StataCorp. (2007). StataCorp, College Station, TX, StataCorp LP.
20. Shevchenko,A., Wilm,M., Vorm,O. and Mann,M. (1996) Mass spectrometric sequencing of proteins silver-stained polyacrylamide gels. *Anal. Chem.*, **68**, 850–858.
21. Perkins,D.N., Pappin,D.J., Creasy,D.M. and Cottrell,J.S. (1999) Probability-based protein identification by searching sequence databases using mass spectrometry data. *Electrophoresis*, **20**, 3551–3567.
22. Lidonnici,M.R., Rossi,R., Paixao,S., Mendoza-Maldonado,R., Paolinelli,R., Arcangeli,C., Giacca,M., Biamonti,G. and Montecucco,A. (2004) Subnuclear distribution of the largest subunit of the human origin recognition complex during the cell cycle. *J. Cell. Sci.*, **117**, 5221–5231.
23. Valacca,C., Bonomi,S., Buratti,E., Pedrotti,S., Baralle,F.E., Sette,C., Ghigna,C. and Biamonti,G. (2010) Sam68 regulates EMT through alternative splicing-activated nonsense-mediated mRNA decay of the SF2/ASF proto-oncogene. *J. Cell. Biol.*, **191**, 87–99.
24. Li,X. and Manley,J.L. (2006) Cotranscriptional processes and their influence on genome stability. *Genes Dev.*, **20**, 1838–1847.
25. Loomis,R.J., Naoe,Y., Parker,J.B., Savic,V., Bozovsky,M.R., Macfarlan,T., Manley,J.L. and Chakravarti,D. (2009) Chromatin binding of SRp20 and ASF/SF2 and dissociation from mitotic chromosomes is modulated by histone H3 serine 10 phosphorylation. *Mol. Cell.*, **33**, 450–461.
26. Shepard,P.J. and Hertel,K.J. (2009) The SR protein family. *Genome Biol.*, **10**, 242.
27. Misteli,T., Caceres,J.F. and Spector,D.L. (1997) The dynamics of a pre-mRNA splicing factor in living cells. *Nature*, **387**, 523–527.
28. Ghigna,C., Giordano,S., Shen,H., Benvenuto,F., Castiglioni,F., Comoglio,P.M., Green,M.R., Riva,S. and Biamonti,G. (2005) Cell motility is controlled by SF2/ASF through alternative splicing of the Ron protooncogene. *Mol. Cell.*, **20**, 881–890.
29. Shultz,J.C., Goehe,R.W., Wijesinghe,D.S., Murudkar,C., Hawkins,A.J., Shay,J.W., Minna,J.D. and Chalfant,C.E. (2010) Alternative splicing of caspase 9 is modulated by the phosphoinositide 3-kinase/Akt pathway via phosphorylation of SRp30a. *Cancer Res.*, **70**, 9185–9196.
30. Karni,R., de Stanchina,E., Lowe,S.W., Sinha,R., Mu,D. and Krainer,A.R. (2007) The gene encoding the splicing factor SF2/ASF is a proto-oncogene. *Nat. Struct. Mol. Biol.*, **14**, 185–193.
31. Hickson,I., Zhao,Y., Richardson,C.J., Green,S.J., Martin,N.M., Orr,A.I., Reaper,P.M., Jackson,S.P., Curtin,N.J. and Smith,G.C. (2004) Identification and characterization of a novel and specific inhibitor of the ataxia-telangiectasia mutated kinase ATM. *Cancer Res.*, **64**, 9152–9159.
32. Kastan,M.B. and Bartek,J. (2004) Cell-cycle checkpoints and cancer. *Nature*, **432**, 316–323.
33. Fernandez-Capetillo,O., Lee,A., Nussenzweig,M. and Nussenzweig,A. (2004) H2AX: the histone guardian of the genome. *DNA Repair*, **3**, 959–967.
34. Dutertre,M., Sanchez,G., Barbier,J., Corcos,L. and Auboeuf,D. (2011) The emerging role of pre-messenger RNA splicing in

stress responses: Sending alternative messages and silent messengers. *RNA Biol.*, **8**, 740–747.
35. Aguilera,A. and Gomez-Gonzalez,B. (2008) Genome instability: a mechanistic view of its causes and consequences. *Nat. Rev. Genet.*, **9**, 204–217.
36. Solier,S., Barb,J., Zeeberg,B.R., Varma,S., Ryan,M.C., Kohn,K.W., Weinstein,J.N., Munson,P.J. and Pommier,Y. (2010) Genome-wide analysis of novel splice variants induced by topoisomerase I poisoning shows preferential occurrence in genes encoding splicing factors. *Cancer Res.*, **70**, 8055–8065.
37. Paulsen,R.D., Soni,D.V., Wollman,R., Hahn,A.T., Yee,M.C., Guan,A., Hesley,J.A., Miller,S.C., Cromwell,E.F., Solow-Cordero,D.E. *et al.* (2009) A genome-wide siRNA screen reveals diverse cellular processes and pathways that mediate genome stability. *Mol. Cell.*, **35**, 228–239.
38. Sun,S., Zhang,Z., Sinha,R., Karni,R. and Krainer,A.R. (2010) SF2/ASF autoregulation involves multiple layers of post-transcriptional and translational control. *Nat. Struct. Mol. Biol.*, **17**, 306–312.
39. Lund,M.K., Kress,T.L. and Guthrie,C. (2008) Autoregulation of Npl3, a yeast SR protein, requires a novel downstream region and serine phosphorylation. *Mol. Cell. Biol.*, **28**, 3873–3881.
40. Begley,T.J., Rosenbach,A.S., Ideker,T. and Samson,L.D. (2002) Damage recovery pathways in Saccharomyces cerevisiae revealed by genomic phenotyping and interactome mapping. *Mol. Cancer Res.*, **1**, 103–112.
41. Smolka,M.B., Albuquerque,C.P., Chen,S.H. and Zhou,H. (2007) Proteome-wide identification of in vivo targets of DNA damage checkpoint kinases. *Proc. Natl Acad. Sci. USA*, **104**, 10364–10369.
42. Chiodi,I., Corioni,M., Giordano,M., Valgardsdottir,R., Ghigna,C., Cobianchi,F., Xu,R.M., Riva,S. and Biamonti,G. (2004) RNA recognition motif 2 directs the recruitment of SF2/ASF to nuclear stress bodies. *Nucleic Acids Res.*, **32**, 4127–4136.
43. Chalfant,C.E., Ogretmen,B., Galadari,S., Kroesen,B.J., Pettus,B.J. and Hannun,Y.A. (2001) FAS activation induces dephosphorylation of SR proteins; dependence on the de novo generation of ceramide and activation of protein phosphatase 1. *J. Biol. Chem.*, **276**, 44848–44855.
44. Lareau,L.F., Inada,M., Green,R.E., Wengrod,J.C. and Brenner,S.E. (2007) Unproductive splicing of SR genes associated with highly conserved and ultraconserved DNA elements. *Nature*, **446**, 926–929.
45. Munoz,M.J., Perez Santangelo,M.S., Paronetto,M.P., de la Mata,M., Pelisch,F., Boireau,S., Glover-Cutter,K., Ben-Dov,C., Blaustein,M., Lozano,J.J. *et al.* (2009) DNA damage regulates alternative splicing through inhibition of RNA polymerase II elongation. *Cell*, **137**, 708–720.